

Review



Cite this article: Labay-Mora A, García-Beni J, Giorgi GL, Soriano MC, Zambrini R. 2024 Neural networks with quantum states of light. *Phil. Trans. R. Soc. A* **382**: 20230346.
<https://doi.org/10.1098/rsta.2023.0346>

Received: 27 May 2024
Accepted: 12 August 2024

One contribution of 18 to a theme issue ‘The quantum theory of light’.

Subject Areas:

quantum physics, quantum computing, artificial intelligence

Keywords:

quantum machine learning, quantum optics, squeezing

Authors for correspondence:

Roberta Zambrini
e-mail: roberta@ifisc.uib-csic.es
Adrià Labay-Mora
e-mail: alabay@ifisc.uib-csic.es

[†]These authors contributed equally to the study.

Neural networks with quantum states of light

Adrià Labay-Mora[†], Jorge García-Beni[†], Gian Luca Giorgi, Miguel C. Soriano and Roberta Zambrini

Institute for Cross-Disciplinary Physics and Complex Systems (IFISC) UIB-CSIC, Campus Universitat Illes Balears, Palma de Mallorca 07122, Spain

id AL-M, 0000-0002-3443-4929; JG-B, 0009-0002-2843-9093; GLG, 0000-0003-3113-0193; MCS, 0000-0002-6140-8451; RZ, 0000-0002-9896-3563

Quantum optical networks are instrumental in addressing the fundamental questions and enable applications ranging from communication to computation and, more recently, machine learning (ML). In particular, photonic artificial neural networks (ANNs) offer the opportunity to exploit the advantages of both classical and quantum optics. Photonic neuro-inspired computation and ML have been successfully demonstrated in classical settings, while quantum optical networks have triggered breakthrough applications such as teleportation, quantum key distribution and quantum computing. We present a perspective on the state of the art in quantum optical ML and the potential advantages of ANNs in circuit designs and beyond, in more general, analogue settings characterized by recurrent and coherent complex interactions. We consider two analogue neuro-inspired applications, namely quantum reservoir computing and quantum associative memories, and discuss the enhanced capabilities offered by quantum substrates, highlighting the specific role of light squeezing in this context.

This article is part of the theme issue ‘The quantum theory of light’.

1. Introduction

Our understanding of the physical properties of light has been transformed by the advent of quantum

mechanics in the early twentieth century and has played a key role in both the first and second quantum revolutions. The theoretical framework of quantum light [1] has been growing and experimentally tested in light–matter interaction, with states of light with no classical analogue, enabling several quantum technologies [2–4]. Quantum optics has played an important role in testing the foundations of quantum mechanics as the particle-wave duality and non-locality [5]. The first observed non-classical state was demonstrated in quantum optics for the predicted phenomenon of squeezed light [6]. This was achieved in the 1980s through experiments that showcased the squeezing of quantum fluctuations in one of the quadratures of the electromagnetic field below the vacuum level, leading to reduced noise in that particular quadrature [7]. Squeezed light has since become a foundational element in numerous applications, playing a crucial role in fields such as precision measurements, quantum information processing and quantum metrology [8]. For instance, squeezed vacuum states were recently employed in the laser interferometer gravitational-wave observatory (LIGO) to mitigate the effect of noise on the readout photodetectors, which resulted in a broadband detection enhancement from tens of hertz to several kilohertz [9]. Quantum optics experiments have also proven instrumental in addressing fundamental questions about the nature of reality, locality and causality. For instance, tests of Bell's inequalities with photons have been instrumental in laying the ground for the study of the non-local nature of quantum entanglement [10].

In the last two decades, single-mode and two-component systems have been successfully scaled to multipartite quantum states, where each mode of the electromagnetic field represents a quantum node that can be coupled with others (via light–matter interaction) to form a complex network. This is the field of multimode quantum optics, which is paving the way to optical quantum networks [11]. Successful implementations of these more complex multi-mode quantum light states triggered pioneering applications in quantum teleportation, quantum key distribution, quantum computing and quantum sensing [2,3]. Generally, quantum technologies overcome, if not lack, direct classical counterparts, being based on inherently quantum phenomena. Still, technologies based on light quantum features often build upon classical optical techniques, leveraging the advantages of both classical and quantum optics. For instance, while quantum techniques such as entanglement-enhanced metrology offer novel capabilities, classical metrology techniques using light-based instruments, such as interferometers, have long been employed for precise measurements. Quantum communication protocols rely on quantum states of light, but transmission using classical light signals in fibre optics is an established technology [12]. More recently, the potential of quantum optics for neuro-inspired ML and ANN started to be explored, leveraging the advantages of both classical and quantum optics.

The scope of this work is to provide a brief perspective of the developments towards quantum optical ANN, inspired, on the one hand, by successful implementations of photonic ML in (classical) devices and, on the other hand, by the unique capabilities of quantum computation and simulation and advances in optical quantum networks. These advances in quantum complex networks and photonic ML set the ground for recent proposals of quantum optical ANN and are briefly reviewed. The relevance of quantum optical complex networks in fundamental questions and different applications—in communication and computation—is presented in §2. Photonic ML *for* (§3) and *with* (§4) quantum optics are then introduced, the latter being our focus. Photonic implementations of computation and ML approaches have been successfully demonstrated in classical settings (§4a), and several advantages have been reported. Quantum implementations can enhance the capabilities of quantum neural networks, both in circuits and in more general (analogue) settings characterized by recurrent and coherent complex interactions (§4b). Two examples of application, namely quantum reservoir computing (QRC) and quantum associative memory (QAM), are discussed in §5, highlighting the role of squeezing in enhancing their performance.

2. Quantum optical networks

Observations of phenomena such as squeezing, anti-bunching and entanglement have been instrumental in establishing the fundamental differences between classical and quantum systems and, thus, the success and importance of quantum optics [1]. While originally considered for one or a few sub-systems, such as two entangled polarizations or frequency components in parametric down-conversion, optical implementations are well suited for scaling to larger multi-mode configurations [1,11], providing an insightful and diverse realization of quantum networks [13]. The transition to large systems with many interacting (optical) components allows not only a broader approach to fundamental questions and quantum information but also breakthrough applications in quantum computing, quantum information processing, secure communications and precision measurement, as shown in the following selected examples. We will highlight different problems and implementations enabled by quantum optical networks of different nature that can be relevant in the context of quantum ANN. A broader review of complex quantum networks beyond optical implementations is presented in [13], describing quantum dynamics in networks, network representations of states, set-ups or dynamics (also beyond photonics).

(a) Fundamental questions

(Quantum) optical networks offer a clear advantage with respect to other platforms in terms of scalability. Spatially multimode beams [14] and frequency combs [15] (broad-spectrum light beams composed of equidistant narrow lines) are outstanding examples. These light fields are very suitable to generate multiphoton entangled states that can also be used as the fundamental brick of a complex network [16–18]. Quantum states of light of increasing complexity [19] can also be generated linearly by injecting photons in (large) interferometers, successfully implemented in integrated photonics [20]. All these quantum optical networks can be used to address different fundamental questions, and in the following, we give a few examples, namely the quantumness certification of complex network states, collective phenomena as spontaneous patterns, synchronization or time crystals and controllable simulation of open quantum systems.

Quantum optics is at the heart of the developments of quantum information of the last half-century. A significant challenge in the field of quantum information science is the development of effective methods for certifying the correct functioning of complex quantum devices. In essence, the issue can be summarized as the necessity to guarantee that quantum devices that would be classically intractable perform according to the predictions of quantum physics [21]. In the context of quantum optical networks, an efficient certification method for multimode pure Gaussian states and non-Gaussian states generated by linear-optical circuits was proposed [22]. Another remarkable example in this direction can be found looking at the fundamental problem of certifying the non-classicality of an entire network, going beyond the violation of Bell inequalities between one pair of parties. A proof-of-principle experimental realization of such protocol was reported in [23], where full network non-locality was shown in a photonic star-shaped network consisting of three entangled photon pairs. A proposal for self-testing all entangled states in a network was presented in [24], which is feasible with current technology.

Optical systems also provide an outstanding platform for exploring the emergence of collective phenomena addressing the quantum aspects [25]. Indeed, combining driving (e.g. by a laser field), dissipation (e.g. in cavities) and (light–matter) interactions in an open quantum system (which can be either a many-body system or a nonlinear oscillator) can give rise to a plethora of phenomena, such as quantum symmetry breaking and dissipative phase transitions. Quantum optics is the natural ground to observe spatio-temporal phenomena such as spontaneous patterns in multimode settings [26], quantum synchronization [27,28], metastability [29] and time crystals [30–32].

Complex quantum networks can also be designed to model engineered and tunable environments, enabling the simulation of a variety of open quantum system dynamics, which allows the study of fundamental issues such as dissipation, decoherence and measurement. It was shown that typical features of open quantum system dynamics such as the spectral density or quantum non-Markovianity can be implemented in a CV optical platform using multimode light, with squeezing and entanglement as resources [33,34]. A proof-of-concept of this controllable dissipation implementation has been recently reported in [35], where such complex networks were experimentally implemented using frequency-combs squeezed light.

(b) Quantum internet

The transmission of information via light represents one of the most widely used methods for communication, with optical fibres or satellites to connect remote places. In recent times, the development of quantum computing has raised the possibility of creating a quantum internet—an extension of the actual internet, a set of interconnected quantum devices capable of sending and storing information by using quantum mechanics [36,37]. The change of paradigm from communication between pairs of users to a fully extended network is the necessary ingredient to make such technology appealing for industry and public institutions, beyond the implication for basic science. The quantum internet aims to be more secure than the current Internet with protocols for quantum key distribution that ensure private communication between two parties [38]. Furthermore, it enables the distribution of computation across remote devices, which has applications in quantum sensing [39] and quantum computation [40].

This new approach introduces significant technical and intellectual challenges due to the nature of quantum mechanics and the limitations of noisy intermediate scale quantum (NISQ) technology. A primary challenge is photon loss in transmission channels like optical fibres, which increases exponentially with distance. Classical systems mitigate photon loss by using coherent sources and repeaters for amplification. In contrast, the quantum internet transmits qubits encoded in the amplitude or polarization of single photons, which suffer from decoherence during transmission. Additionally, qubits cannot be cloned [41], necessitating new methods to overcome photon loss. One potential solution is the development of all-photonic quantum repeaters, which eliminate the need for matter quantum memories and achieve a communication efficiency that scales polynomially with the channel distance [42].

Similarly, other protocols for quantum communication implemented using squeezed quantum states of light have gained interest recently due to easier experimental viability in the NISQ era [43]. Compared to discrete variables (DV) quantum key distribution, CV proposals are expected to be more efficient, attain higher rates and improve the detection using homodyne receivers as opposed to single-photon counters [44]. The first proposal used squeezed states [45], which are secure [46] and have been shown to have improved robustness versus the noise of the channel [47].

(c) Quantum computation and simulation

Complex quantum states emerge naturally in quantum computation and simulations both in circuit and analogue implementations [48–50]. In this context, successful photonic realizations have been reported, as reviewed in [51,52]. While quantum computing systems such as superconducting circuits, trapped ions and silicon quantum dots are very popular in state-of-the-art quantum processors, they face challenges in achieving scalable fault tolerance due to fragile quantum states requiring cryogenic or vacuum isolation. Photonic systems, on the other hand, are intrinsically more robust and can be manipulated at room temperature. Photons offer fast propagation and large bandwidth. These properties, together with advanced photon manipulation technologies, position photonic systems as a leading approach for building quantum computers [53].

One of the ways of implementing universal photonic quantum computing in CV is measurement-based quantum computing, where cluster states are used as a resource to perform CV gates by applying local operations thanks to quantum teleportation protocols [54]. This framework enables extremely high scalability and reconfigurability, mainly using temporal and frequency mode multiplexing [18,55–57]. Deterministic single- and multi-mode gates are within current experimental reach [58,59], which is an advantage compared with probabilistic gates in DVs schemes [60]. The main limitation of CV measurement-based quantum computing is the implementation of single cubic phase gates, which are a requirement for universality [54]. Advances in hybrid discrete-CV implementations have been done to address this limitation [61].

In the search for fault-tolerant quantum computation, quantum error correction is necessary to prevent the propagation of logical errors in operations. Qubit-based quantum error correction techniques are challenging to implement due to the difficulties in scaling up the number of qubits [62]. Photonic quantum computers also allow the implementation of efficient error correction codes that exploit the infinite-dimensional Hilbert space of CV to encode a qubit in single optical modes, thus simplifying the scalability of error correction [63]. Hence, by exploiting the redundancy of the Hilbert space, quantum error correction could be constructed in a single bosonic mode. The most notable ones are Gottesman–Kitaev–Preskil (GKP) [64], binomial [65] and cat codes [66]. In particular, cat codes can exponentially suppress bit-flip errors [67], and squeezed-cat codes can enhance the protection against such errors [68].

Photonic architectures have also been successful in implementing non-universal computing tasks. Boson sampling is one of the most prominent applications of quantum photonic hardware in this regard, as photonic networks generated with large interferometers cannot be efficiently simulated by classical computers [69]. Gaussian boson sampling represents a specialized model of photonic quantum computation [70]. It involves the preparation of a multi-mode squeezed state followed by measurements conducted on the Fock basis. The primary distinction from universal photonic circuits lies in the absence of non-Gaussian gates within Gaussian boson sampling and the limitation of measurements to the Fock basis. Quantum advantage has been successfully achieved in Gaussian boson sampling using specifically built photonic hardware [71,72], as well as in a reconfigurable platform built by Xanadu [73]. Quantum squeezed states have also found applications in the design of high-dimensional coherent Ising machines [74,75], which are suited to solve complex combinatorial optimization problems. Another technique to solve such problems is quantum annealing which has been seen to be more robust to noise and allows for all-to-all connectivity when qubits are encoded in the ground states of Kerr parametric oscillators [76,77]. Furthermore, photonic quantum processing units were used to efficiently solve the quantum phase estimation algorithm through a variational eigensolver algorithm [78].

Advances in scalable, efficient and fast, photonic architectures enable the generation of quantum optical networks that open new frontiers also in the rapidly evolving fields of ML and neuro-inspired computation, as presented in §4. Interestingly, the same developments in these quantum optical complex architectures have also benefited from the use of ML methods, and some examples are given in §3.

3. Machine learning for quantum optics

The use of ML techniques to enhance classical optical systems is rapidly advancing, achieving a high degree of sophistication [79,80]. ML is being employed in various applications, such as controlling experimental instabilities, designing novel devices with ad-hoc functionalities and generating ultrafast optical pulses. For instance, genetic algorithms can predict and mitigate fluctuations in optical experiments, leading to more stable and reliable results [81]. Additionally, deep learning techniques enable the design of optical components with customized properties, optimizing performance for specific tasks [82]. ML also plays a crucial role

in the generation and shaping of ultrafast optical pulses, which are essential for applications ranging from telecommunications to medical imaging [79]. Overall, the integration of ML in classical optics enhances existing technologies and also clears the way for innovative solutions and discoveries.

As photonic hardware for quantum optics advances, optimizing optical setups for specific applications becomes increasingly challenging, prompting a shift from manual design by scientists to automated methods using ML [83]. ML can significantly enhance quantum photonic protocols by optimizing parameters, accelerating measurements and eliminating systematic artefacts, thus enabling configurations previously untestable due to experimental limitations. Furthermore, such automatic exploration methods have already facilitated the creation of novel quantum photonic setups and the discovery of new photonic phenomena, highlighting their transformative potential in this field [84]. In these approaches, quantum photonic experiments are recast into graph representations [83], allowing the task of finding structures in a given graph to be translated into discovering new experimental setups [85]. Ideally, these methods for automated design can also offer a better conceptual understanding [86].

Machine learning can also assist in the development of a quantum internet, highly dependent on the interplay between the various building blocks that make up the network, from the hardware used for quantum computers or transmission channels to the protocols used to distribute entanglement among distant nodes or generate secret keys [60]. Finding the optimal hardware and software parameters that allow optimal connectivity is a huge computational problem, especially in the NISQ era. In this context, analytical solutions are difficult to find, and one has to resort to optimization algorithms to find more general solutions [87,88]. ML can be used to find better protocols, optimize hardware parameters or improve the security and transmission rates of quantum key distribution [89].

Another challenge in many quantum technologies is the full reconstruction (tomography) of a quantum state, which is one of the most resource-consuming tasks. As shown in [90], trained ANNs provide a simple and adaptable method for quantum state tomography, effectively utilizing a limited amount of experimental data. An example of the potential for neural networks to assist in the extraction of relevant features from a multipartite quantum state of light was recently reported in [91]. The degree of entanglement was quantified without the need to know the full description of the quantum state, achieving an error of up to an order of magnitude lower than the state-of-the-art quantum tomography. Finally, quantum imaging has also greatly benefited from the application of ML algorithms. For instance, deep neural networks have been proven effective in a diversity of imaging applications, ghost imaging or phase retrieval, as experimentally shown in [92].

4. Photonic neural networks

Photonic quantum technologies represent a promising opportunity to address the demand for fast processing, high performance and energy efficiency in classical and also quantum data processing. As presented in the following (§4a), classical optical systems have already enabled successful implementations of landmark results. Proposals exploring designs and applications of ANNs based on quantum states of light are then introduced, both in feed-forward circuit approaches and beyond and in particular in QRC and QAM (§4b).

(a) Machine learning with classical light

Optical ML and the dominant approach of ANNs harness the unique properties of light to achieve unprecedented speeds and efficiencies in information processing. Classical optical computing, which exploits principles such as light propagation and interference, is

experiencing a resurgence as a powerful alternative to traditional electronic computation [93]. This renewed interest is driven by significant advancements in photonic technologies and the increasing demand for more efficient and faster computing methods [94].

Optical neural networks (ONNs) can exploit the inherent properties of light, such as coherence, interference and diffraction, to implement physical analogues of ML algorithms [95,96]. Utilizing the vast bandwidth of optical frequencies, ONNs enable parallel processing of large amounts of data, making them suitable for complex ML tasks. Recent review and perspective articles highlight foundational principles and recent advancements, underscoring the transformative potential of classical optics in neural network architectures [97–99] based on linear and nonlinear elements such as Mach–Zehnder interferometers and saturable absorbers [95,100].

The advantages of optical systems in ML are numerous [93]. All-optical computing systems can potentially outperform electronic and optoelectronic counterparts in terms of energy consumption and scalability [101]. This efficiency stems from the minimal energy dissipation in optical fibres and waveguides compared with electronic circuits. Additionally, the integration of optical components on a large scale enhances scalability, making these systems suitable for extensive neural network implementations [102,103]. The inherent high-speed nature of light facilitates rapid data processing and low latency, which is crucial for real-time ML applications [104].

Moving to the quantum regime, the advantages of optics for classical ML are inherited as illustrated in figure 1. Furthermore, as common also in other ML settings, the enlarged Hilbert space has the potential to boost the performance (e.g. exponentially increasing the expressivity), and a quantum approach enables the processing of quantum inputs, efficiently executing quantum tasks. Major limitations of quantum technologies caused by decoherence due to the effect of the environment are alleviated for quantum states of light, which exhibit entanglement and noise below the familiar shot noise (squeezing) even at room temperatures. Among the challenges is the inefficiency of light signal interactions at low intensities, which can be overcome with different strategies paving the way for robust and versatile quantum optical ML systems.

(b) Quantum neural networks architectures

Successful implementations of quantum computation and simulations, landmark experiments in quantum optics (§2) and recent advance of ML, even with classical light, hints at the potential high performance of quantum machine learning with quantum optical settings. The first proposed designs of quantum neural networks have been inspired by classical feed-forward neural networks with a sequence of unitary gates acting on different layers [105]. These ANN circuits are based on a sequence of generally local operations. Alternative designs are instead inspired by recurrent neural networks, implemented to the coherent interaction between different components in complex interacting systems, being associated with analogue designs common in quantum simulations. This distinction between circuit and analogue design in quantum neuromorphic computing has been recently reviewed in [106], comparing approaches based on parameterized quantum circuits, with others based on quantum oscillator networks to compute, closer to classical neuromorphic computing. Focusing on photonic quantum ANN, there have been recent proposals in both analogue and circuit platforms, encompassing a broad spectrum of designs that also includes both CV [107] and DVs [108].

Quantum ANN based on variational quantum circuits has been the primary focus in the quantum ML community [109,110] impulsed by the development of state-of-the-art superconducting gate-based circuits NISQ computers. A variational quantum circuit consists of a sequence of unitary operations with adjustable parameters, typically used within hybrid quantum-classical algorithms, where a classical optimizer iteratively tunes these parameters to minimize a cost function related to a specific problem. In the last few years, these circuit-based,

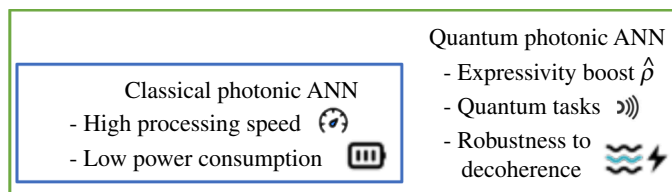


Figure 1. Schematic visualization of the main advantages of classical photonic ANNs, which are inherited by the quantum counterparts. Quantum photonic ANNs have in addition access to a large Hilbert space with the potential for an exponential expressivity boost, exhibit a strong robustness to decoherence and can efficiently embed quantum states and tasks, as, e.g. entanglement detection or quantum sensing.

feed-forward neural networks have been studied in integrated photonic-based platforms, often structured as regular deep ANN. The linear neuron connections are realized with linear optical components while the nonlinear neuron activation often relies on quantum measurement. In [108], the concept of a quantum ONN was proposed to demonstrate that quantum optical phenomena can be integrated into neural networks. The considered platform consists of inputs in single-photon Fock states, variational linear optics operation circuits, single-site Kerr-type nonlinearities and photon-number-resolving detectors. This framework has been expanded to quantum convolutional neural networks [111]. Neural networks based on variational quantum circuits within the CV architecture have been studied in [107], where electromagnetic field amplitudes encode quantum information. The layered structure consists of continuously parameterized Gaussian and non-Gaussian gates, universal for CV quantum computation. Applications discussed include fraud detection, image generation and hybrid classical-quantum autoencoders. Circuit-based implementations have also been proposed in the context of Associative Memory (AM) as variations of Grover's search algorithm [112]. While these models are useful in certain use cases [113,114], they deviate from the original idea, where a dynamical system is the resource that performs the association process. A more general overview of classical and quantum AM is presented below.

Beyond sequential circuit architectures, quantum ANN have been considered in different proposals based on quantum optical networks in recurrent instead of deep feed-forward designs. Recurrent neural networks do naturally arise considering the coherent interactions in complex quantum systems and have been recently considered in different proposals [115–117]. In [115], optimization of a network of oscillators in CV enables online quantum time series processing. Training all internal interactions, it was possible to entangle sequential inputs at different times. Delay lines have been added leading to memory modes as a quantum optical recurrent neural network, and a proof-of-concept implementation has been realized [116] on the photonic processor Borealis [73].

A less demanding architecture of quantum ONN not restricted to circuit design (but also suitable for quantum computing [118–120]) and requiring reduced optimization resources are extreme learning machines and more generally, QRC [117]. Pioneered by the work of Fujii and Nakajima in 2017 [121], QRC has gained traction as a wider range of quantum substrates has been explored [117]. Reservoir computing originated as a classical ML paradigm that simplifies the training of recurrent neural networks [122]. It has since become an umbrella term for algorithms and physical systems that exploit random (non-optimized) dynamical systems for ML tasks [123]. In particular, classical photonic implementations of reservoir computing are becoming increasingly popular for ultra-fast information processing applications being particularly suited for temporal data and memory tasks [124].

Quantum optical platforms have also found their applications in this ML framework, either in DVs [125–128], CV [129–132] or hybrid qubit-photonic schemes [133,134]. QRC in DVs has been proposed in integrated photonic circuits using a novel quantum memristor to add memory and nonlinearities to the quantum dynamics, via the measurement back action [125]. Considering instead continuously coupled bosonic networks with hopping Hamiltonians, the

larger Hilbert space yields performance improvements, exploiting the larger system expressivity [126]. Time series processing was also demonstrated in a proposal based on photon detection of a quantum oscillator dimer in [127].

Moving to CV platforms, a single quantum oscillator with a Kerr nonlinearity was shown to achieve the estimation of the phase of a classical signal with lower error than a classical setting [129]. The first CV proposal based on quantum oscillator networks in Gaussian states and homodyne detection was proposed in [130], in which saturation of polynomial scaling was also demonstrated. This was extended to an experimental design considering multimode pulses recirculating through a closed cavity loop coupled to an external signal [131]. Real-time processing through physical ensembles [131] and cavity squeezing for noise robustness [132] were also studied. Recently, the first experimental implementation of an analogue QRC has been reported in a hybrid qubit-CV setup [134], where microwave signals were used as input to feed a reservoir made of a quantum superconducting circuit comprising a linear oscillator coupled to a single qubit.

Also AM can be implemented in quantum neural networks that go beyond circuit designs and quantum computation. AM arises when a system is able to retrieve the correct pre-stored memory or *pattern* once interrogated with corrupted or partial initial information. AMs are commonly modelled through the (classical) Hopfield neural network [135] consisting of an all-to-all network of classical spins, modelling neurons in active (+1) or inactive (−1) states, which evolve to minimize a given energy function through repeated network updates. This drives the system to settle into one of many stable spin configurations, the one associated with a stored memory or pattern. Here, patterns correspond to strings of classical bits which are written, through a proper *learning rule*, in the weights of the neural connections [136]. In the spirit of Hopfield, analogue implementations of QAM in open quantum systems allow spanning a manifold of stable states that can be identified as patterns. Here, generalizations of the Hopfield neural network range from binary neurons to qudits, in both closed [137,138] and open quantum systems [139–141]. Some analogue approaches deal with the derivation of effective QAM models that exploit a quantum substrate, e.g. multimode Dicke models [142], confocal cavity QED systems [143], to embed patterns via classical learning rules. All previous work relies on the classical Hebbian learning rule which limits the amount of patterns stored in the system [144]. However, recent models compatible with generic quantum neural networks seem to identify a potential quantum advantage [145]. Retaining Hopfield's original idea, Labay-Mora *et al.* [146] propose the use of a single driven-dissipative quantum resonator which increases the storage capacity of classical AM. Still, these proposals are limited to the storage of classical-like patterns. In §5b, we will study a system where patterns are encoded in genuine quantum states of light.

5. Squeezing in quantum photonic artificial neural networks

As discussed in previous sections, squeezing—a quantum phenomenon reducing light field quadrature fluctuations below shot noise levels—has advanced from fundamental tests like EPR paradox experiments to key applications in quantum technologies [1]. It enhances measurement sensitivity in quantum metrology [8], clock synchronization [147] and gravitational wave detection [9], supports quantum cryptography [148] and enables quantum advantage in Gaussian boson sampling [71–73]. Moreover, squeezing is vital for universal measurement-based quantum computing in CVs [55,57–59] and enables CV quantum ANNs in quantum ML [107,130].

We can characterize squeezed states by the quadrature fluctuations $\langle (\Delta \hat{X}_\theta)^2 \rangle = \langle \hat{X}_\theta^2 \rangle - \langle \hat{X}_\theta \rangle^2$ where $\hat{X}_\theta = [\hat{a} \exp(-i\theta) + \hat{a}^\dagger \exp(i\theta)]/\sqrt{2}$ [6]. Here, the angle θ is the direction where the quadrature fluctuations are measured. The operators \hat{a} and \hat{a}^\dagger are the annihilation and creation operators, respectively, and commonly used quadratures are the position \hat{x} and momentum \hat{p} quadrature—as $\hat{x} = \hat{X}_0$ and $\hat{p} = \hat{X}_{\pi/2}$. If we choose θ as the angle of minimum fluctuations θ^* ,

then a state is squeezed if its fluctuation goes below the vacuum variance (shot noise limit) $\langle(\Delta\hat{X}_{\theta^*})^2\rangle < s_{\text{vac}}^2 = 0.5$. Another quantity that can be used to classify squeezed states is Mandel's Q parameter [1]

$$Q = \frac{\langle(\Delta\hat{n})^2\rangle - \langle\hat{n}\rangle}{\langle\hat{n}\rangle}, \quad (5.1)$$

where $\hat{n} = \hat{a}^\dagger\hat{a}$ is the photon-number operator. The Mandel parameter classifies quantum states as sub-Poissonian ($-1 \leq Q < 0$) and super-Poissonian ($Q > 0$), with coherent states ($Q = 0$) displaying a Poisson distribution with a mean photon number equal to their variance.

In the following, we will explore two use cases of squeezed states for quantum ML. In the first, we will present a platform that realizes a quantum photonic recurrent ANN, taking advantage of squeezing to implement nonlinearity through input encoding and improving the performance of a forecasting task in QRC. In the second, we analyse how squeezed states perform in QAM tasks, demonstrating the use of real quantum states to store quantum patterns.

(a) Quantum reservoir computing

Recent advances in analogue CV quantum networks applied to QRC have demonstrated the potential of using squeezed states of light to improve performance. Input auxiliary squeezed states are a way to introduce nonlinearity in the input encoding of quantum oscillator networks, since the inherent dynamics of Gaussian states are linear in the quadrature operators [130,149]. An advantage of using squeezed state encoding over coherent state encoding is the access to the broader Hilbert space of quantum correlations contained in the covariance matrix of the quantum reservoir [130]. In later proposals consisting of multimode pulses, the encoding of classical signals in the squeezing phase of the input vacuum states was also used to obtain nonlinearities in the output observables [131,132]. Another advantage of squeezed input states is that, because the information is encoded in the quantum fluctuations, information processing can be performed while the quantum reservoir is in a vacuum state of zero mean field amplitude. Comparing with classical states of zero mean amplitude, such as thermal states with input encoded in the thermal excitations, only linear memory in the readout observables is displayed while nonlinear memory is achieved in the presence of squeezing and either amplitude or phase encoding [130]. Squeezing is not only beneficial for the nonlinearity in the input layer encoding, but it has also been shown to improve the noise robustness of photonic QRC platforms when incorporated into the reservoir dynamics [132]. In photonic quantum reservoirs with coherent feedback loops in the form of a cavity, the squeezing produced by the cavity has been shown to be a useful resource for improving the noise resilience of the protocol. In realistic scenarios, noise fluctuations are present throughout the protocol, with those affecting readout measurements being the most detrimental to QRC performance [150].

The quantum reservoir under consideration is similar to that described in [132]. The quantum substrate consists of a multimode optical pulse circulating through a closed loop (optical cavity) with a nonlinear crystal that the reservoir pulse passes through on each round trip (as shown in figure 2a). The cavity is connected to the output detector and to the input information via a 50 : 50 beam splitter that couples the reservoir to external engineered pulses. The classical input information to be processed is encoded in these external pulses and fed to the reservoir. The remaining optical path of the beam splitter output, with light exiting the cavity, is used to sequentially monitor the state of the quantum reservoir using multimode homodyne detection of the x -quadratures [151]. The platform has the advantage of having a coherent quantum memory that does not rely on electronic feedback to create a recurrent ANN.

In CV quantum optics, each quantum state is determined by the statistics of its quadrature vector, defined as $\hat{\mathbf{R}} = (\hat{x}_1, \hat{p}_1, \dots, \hat{x}_N, \hat{p}_N)^\top$, \hat{x}_i and \hat{p}_i are the quadrature operators of the i th optical mode contained in the quantum state. Specifically, each of the external engineered

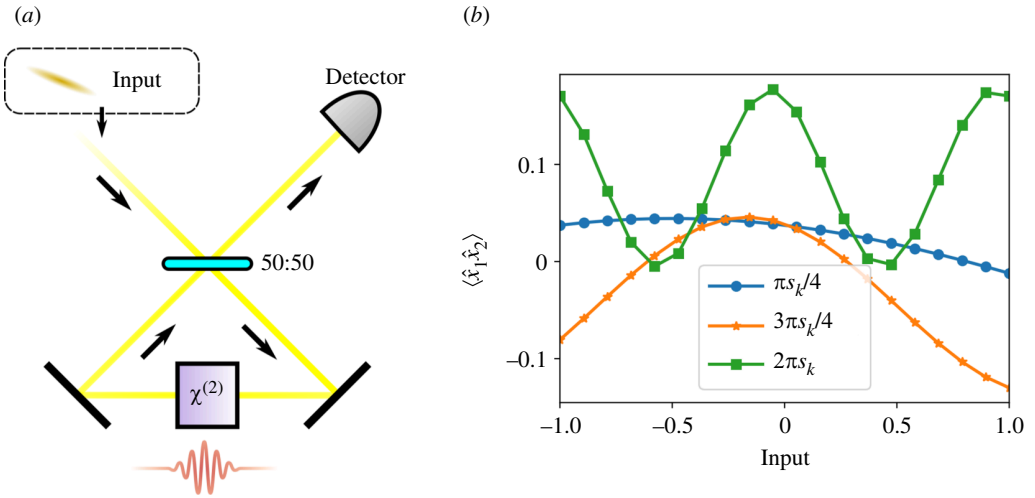


Figure 2. (a) Scheme of a loop-based quantum reservoir. (b) Response of the quantum reservoir to the input at time step k . Here the correlations $\langle \hat{x}_1 \hat{x}_2 \rangle$ are shown for a random but fixed network and input sequence with an $N = 2$ reservoir. Different lines depict different encodings on the squeezing angle of the input states, ϕ_k . The squeezing present in the input states is set at $\xi_{\text{in}} = 0.75$ in equation (5.2) (around -3.3 dB).

pulses that we will couple to the cavity will have a quadrature vector $\widehat{\mathbf{R}}_{\text{in}}^{(k)}$, where the label k stands for the order of the input state in the sequence, so it is a temporal label. Each of them will be the product state of single-mode squeezed states with classical information encoded in their phases. In that way, we can write the covariance matrix of every input state as [152]

$$\text{cov}[\widehat{\mathbf{R}}_{\text{in}}^{(k)}, \widehat{\mathbf{R}}_{\text{in}}^{(k)}] = \bigoplus_{i=1}^N \begin{pmatrix} \cosh(\xi_{\text{in}}) + \cos(\phi_k) \sinh(\xi_{\text{in}}) & \sin(\phi_k) \sinh(\xi_{\text{in}}) \\ \sin(\phi_k) \sinh(\xi_{\text{in}}) & \cosh(\xi_{\text{in}}) - \cos(\phi_k) \sinh(\xi_{\text{in}}) \end{pmatrix}, \quad (5.2)$$

where ξ_{in} stands for the squeezing strength (we consider the same squeezing for every mode), and ϕ_k is the squeezing phase, which is a function of a classical number s_k belonging to the classical input sequence that we want to process. The nonlinear crystal from the cavity applies a quadratic Hamiltonian, which we can write in a generic way as

$$\widehat{H}_{\chi^{(2)}} = \sum_{i,j=1}^N \left(\alpha_{ij} \hat{a}_i^\dagger \hat{a}_j + \beta_{ij} \hat{a}_i^\dagger \hat{a}_j^\dagger + \text{h.c.} \right), \quad (i \geq j) \quad (5.3)$$

with coupling parameters α_{ij} and β_{ij} . If any of the β_{ij} terms are different from zero, the crystal generates squeezing, and this increases the squeezing present in the circulating reservoir pulse. With this set-up, the response of the quantum observables to the classical input fed by the input squeezing phase, ϕ_k from equation (5.2), becomes nonlinear, as can be seen in figure 2b. As shown in this figure, the nonlinearity is not only present but highly tunable by changing the input encoding of the function ϕ_k , which was also illustrated in [131]. This allows a high reconfigurability of the reservoir for different tasks, and comes at a very low experimental cost, as the network is kept fixed at all times.

Going beyond ideal conditions, noise is to be considered in the measured quantities [131,153]. Doing so, at every time step, the measured readout values can be written as

$$\mathbf{O}_{\text{meas}}^{(k)} = \mathbf{O}_{\text{ideal}}^{(k)} + \mathbf{u}(0, s_{\text{noise}}^2), \quad (5.4)$$

where $\mathbf{O}_{\text{ideal}}^{(k)}$ is a vector containing the expected values of the chosen observables in ideal, noiseless conditions, while $\mathbf{O}_{\text{meas}}^{(k)}$ contains the measured observables. The vector $\mathbf{u}(0, s_{\text{noise}}^2)$ resembles the readout noise, which we model as additive Gaussian fluctuations with zero mean and variance equal to s_{noise}^2 added to the quadrature measurements. In our case, the variance of

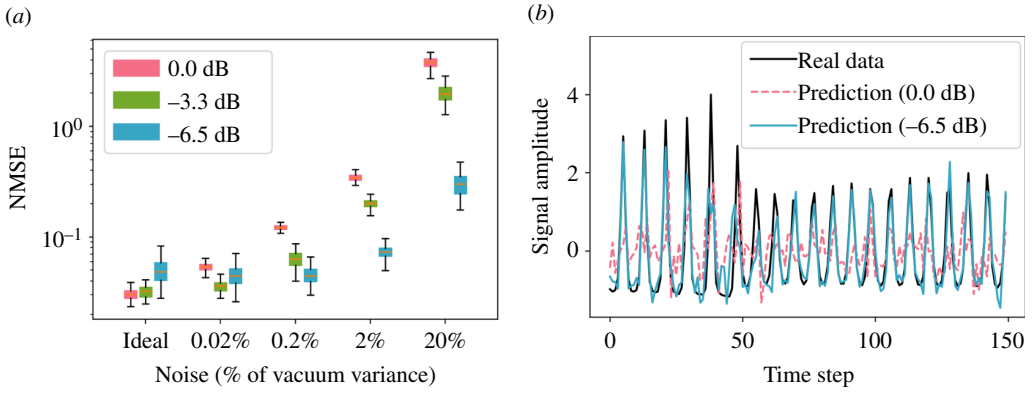


Figure 3. (a) Boxplot of the NMSE for the chaotic time-series forecasting task as a function of the intensity of the added readout noise relative to the vacuum variance. Different colours show different values of the squeezing generated by the nonlinear cavity (from left to right: 0 dB, -3.3 dB and -6.5 dB). Each box contains values from 100 independent realizations. (b) Prediction of the chaotic signal (black) in the presence of high noise (20% vacuum variance intensity) for a reservoir without cavity squeezing (dashed magenta) and for a reservoir with -6.5 dB of cavity squeezing (blue). In all cases, the reservoir had $N = 12$ modes, the input phase encoding was $\phi_k = \pi s_k/4$, the input state squeezing is set at around -3.3 dB, and the nonlinear cavity squeezing is indicated in the figure legends.

the vacuum noise is assumed to be $s_{\text{vac}}^2 = 0.5$, so that we can express the additive noise intensity relative to the vacuum fluctuations. For example, a noise's variance of $s_{\text{noise}}^2 = 0.1$ would be equivalent to a noise with a relative intensity of 20% of the vacuum fluctuations.

For our simulations, the squeezing generated by the Hamiltonian is the same for each mode, which is something we can easily tune using the Bloch-Messiah decomposition [154,155]. We will consider second- and fourth-order moments of the measured x -quadratures, $\{\langle \hat{x}_i \hat{x}_j \rangle, \langle \hat{x}_i^2 \hat{x}_j^2 \rangle, \langle \hat{x}_i^3 \hat{x}_j \rangle\}_{i,j=1}^N$, as outputs for the readout layer ($\langle \cdot \rangle$ stands for the expected values of the observables). The task we consider is the forecasting of the Santa Fe chaotic time series [156,157]. At each time step, we want the reservoir to predict the next step in the series, so the target function is $\bar{y}(s_k) = s_{k+1}$. The data set contains 4000 consecutive values in total, from which we take the training set of 3000 points and the test set of 700 values (the first 300 values are used for the wash-out). We use NMSE as the performance metric that we want to minimize during training. It is defined as $\text{NMSE}(\mathbf{y}, \bar{\mathbf{y}}) = \langle (\mathbf{y} - \bar{\mathbf{y}})^2 \rangle / \langle \bar{\mathbf{y}}^2 \rangle$, where $\bar{\mathbf{y}}$ is the target function vector, and \mathbf{y} are the reservoir predictions. Here, the averages $\langle \cdot \rangle$ are taken among the values of either the training or the test set. In figure 3a, the NMSE is shown as a function of the noise intensity (including the ideal noiseless case) for different values of the generated cavity squeezing (different colours). The squeezing seems detrimental to the performance in ideal and very low noise conditions (noise intensities around and below 0.02% of vacuum noise). However, as the noise increases, the robustness of the reservoir is determined by the amount of squeezing produced by the cavity. In figure 3b, the prediction for a subset of the test values is shown for a single realization of a reservoir considering noisy measurements either with no cavity squeezing (magenta dashed curve) or with ~ 6.5 dB of squeezing (blue curve). The noise conditions are severe (20% of vacuum fluctuations). The difference in prediction power in both scenarios is clearly seen in the figure. However, with such high noise, it is difficult for the reservoir to predict the abrupt change in oscillation amplitude around time step 50 of the chaotic signal, even with high cavity squeezing. These results are consistent with those presented in [132]. Introducing additional squeezing through an active cavity offers enhanced robustness to readout noise. The interplay between linear elements such as the beam splitter setting the number of photons in the loop pulse and the squeezing effect increasing its energy determine the final performance and signal-to-noise ratio in the output layer. Squeezing can

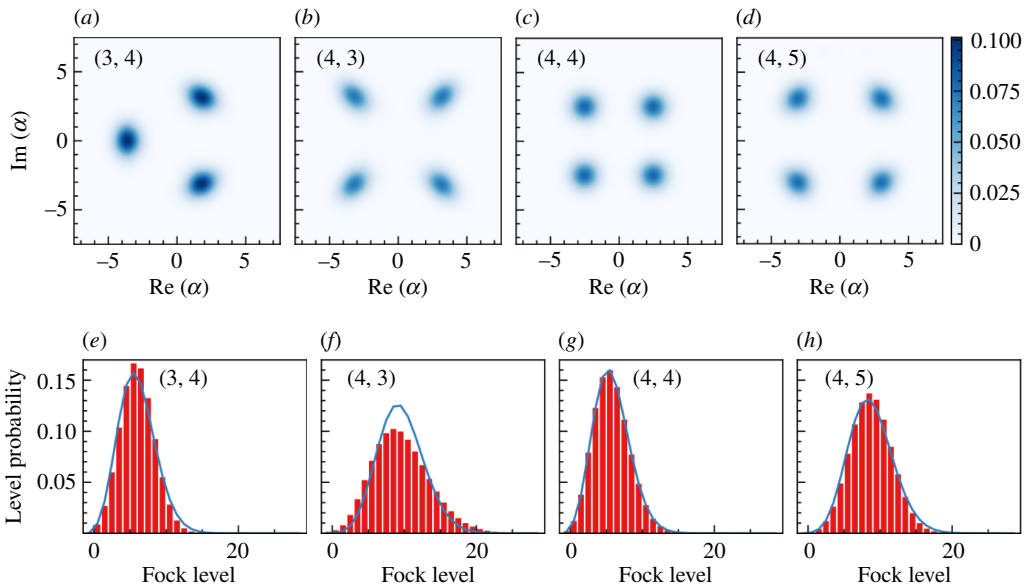


Figure 4. (a–d) Wigner representation of the steady state for different nonlinear degrees. (e–h) Probability distribution of the Fock levels (red histogram) corresponding to the steady states in (a–d), respectively. In blue, the Gaussian distribution of a coherent state with the same mean-photon number. All plots use the same value for $\gamma_m/\gamma_1 = 0.2$ and $\Delta/\gamma_1 = 0.4$, the driving strength for each case is: (a,e) $\eta_3/\gamma_1 = 13.02$, (b,f) $\eta_4/\gamma_1 = 0.8$, (c,g) $\eta_4/\gamma_1 = 3.9$ and (d,h) $\eta_4/\gamma_1 = 91.13$.

counteract the beam-splitter losses and assist in retaining information in the loop pulse for longer, making it more resilient to additive noise.

The proposed platform is not beyond experimental reach with state-of-the-art technologies: necessary tools such as fast squeezing phase setting devices [73,158], reconfigurable network structures from nonlinear sources [18,159] (with some modes reaching squeezing values beyond 6.5 dB [18]) and multimode homodyne detection of multimode pulses [151,160], are within current technological capabilities.

(b) Quantum associative memory

AM models have been explored in the quantum domain with the extension of the classical Hopfield neural network. In these cases, the binary neurons are replaced by two-level quantum systems embedded in a bath, where the classical dynamics is encoded in the jump operators between the system and the bath [139]. Such models give rise to new dynamical phases but cannot improve the memory of classical models [144]. Moreover, these systems only allow the retrieval of patterns encoded in classical states. Enabling information to be encoded in quantum states could open up the possibility of improving performance over classical models. In this respect, we have extended the work introduced in [146], where patterns are encoded in coherent states, to allow for squeezed states [68]. We thus demonstrate the use of bona fide quantum states for memory retrieval.

The system under consideration is a single driven-dissipative nonlinear quantum oscillator, where one can exploit its (in principle infinite) number of degrees of freedom, represented by the density matrix of the system, for computational purposes. Following the intuition of [161], a density matrix itself can be seen as a complex quantum network, whose links are built through the set of bipartite correlations within degrees of freedom, and the complexity of such networks can facilitate the successful achievement of computational tasks [162].

The Gorini–Kossakowski–Sudarshan–Lindblad master equation describing the temporal evolution of the oscillator is

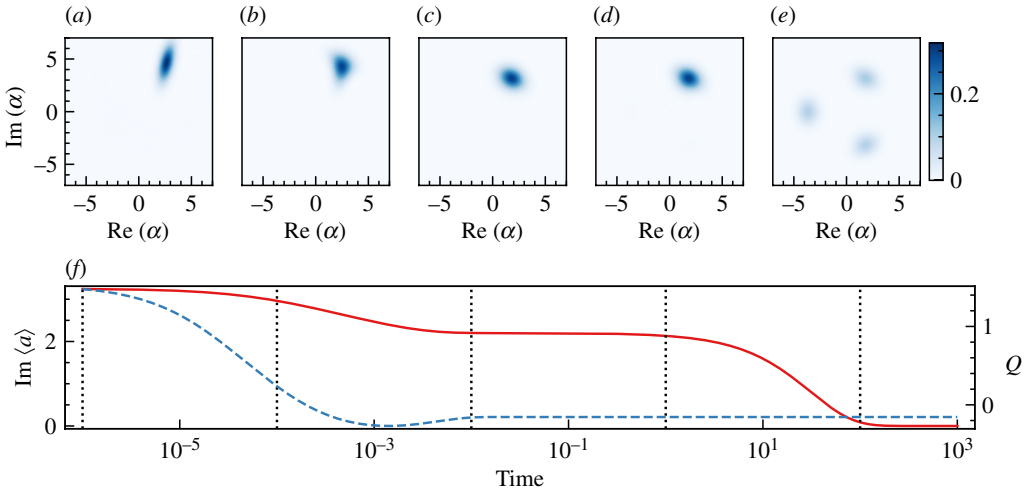


Figure 5. (a–e) Wigner representation of the time evolution of an initial squeezed coherent state with displacement $1.5|\beta_j| \exp(i\pi/3)$ and squeezing parameter $0.5 \exp(-i0.15\pi)$. The times at which the Wigner distribution is calculated correspond to the vertical bars in (f). (f) Evolution of the expectation value of \hat{a} (red solid, left) and the Mandel parameter Q (blue dashed, right). The resonator parameters are: $n = 3$, $m = 4$, $\gamma_4/\gamma_1 = 0.2$, $\eta_3/\gamma_1 = 13.02$ and $\Delta = 0.4$.

$$\frac{\partial \rho}{\partial t} = -i[\hat{H}_n, \rho] + \gamma_1 \mathcal{D}[\hat{a}]\rho + \gamma_m \mathcal{D}[\hat{a}^m]\rho, \quad (5.5)$$

where we have the standard linear (single-photon) damping and an engineered nonlinear (multiphoton) damping [66] with rates γ_1 and γ_m , respectively. The Hamiltonian, which contains an n -order squeezing drive [163], in the rotation frame and after the parametric approximation, is

$$\hat{H}_n = \Delta \hat{a}^\dagger \hat{a} + i\eta [\hat{a}^n - (\hat{a}^\dagger)^n].$$

Here, $\Delta = \omega_0 - \omega_s$ is the detuning between the natural oscillator frequency and that of the squeezing force, and η is the magnitude of the driving.

The main ingredient of our approach lies in the nonlinearity which determines the form and phase symmetry of the steady state, changing from coherent states to purely quantum states, depending on the model parameters. In figure 4a–d, we can see the Wigner representation of the steady state for different combinations of nonlinear degrees (n, m). Due to the rotational \mathbb{Z}_n symmetry of equation (5.5), the steady state is formed by n symmetrically distributed squeezed-coherent states $\{|\beta \exp[i(2j+1)/n], \xi_j]\}_{j=1}^n$ whose shape changes depending on the relation between n and m . Only in the case $n = m$, the lobes are well-described by coherent states ($\xi_j = 0$) as we can appreciate in figure 4c,g where the probability distribution of Fock states follows a Gaussian distribution. In all the other cases, we find squeezed states whose distribution is super-Poissonian for $m < n$ (see figure 4b) or sub-Poissonian for $m > n$ (see figure 4a,d), leading to phase-squeezed and amplitude-squeezed states, respectively. In our case, the amplitude of the lobes can be determined from the oscillator parameters $\beta \approx (2n\eta_n/m\gamma_m)^{1/(2m-n)}$, and the strength of the squeezing $|\xi_j|$ has been seen numerically to depend only on the relation of nonlinear degrees n and m [68].

In addition, this type of resonator has a metastable dynamical phase where the squeezed lobes $\{|\beta_j, \xi_j]\}_{j=1}^n$ become metastable states. The metastable phase is a consequence of a large separation in the Liouvillian spectrum, which divides the dynamics into different timescales where the dynamics are confined for a long time, compared with all timescales, in the metastable manifold spanned by the n metastable states [164]. Concerning AM, metastability allows systems converging to a unique steady state to span a manifold of relevant addressable memories [165]. More specifically, within the metastable transient, an initial state will move

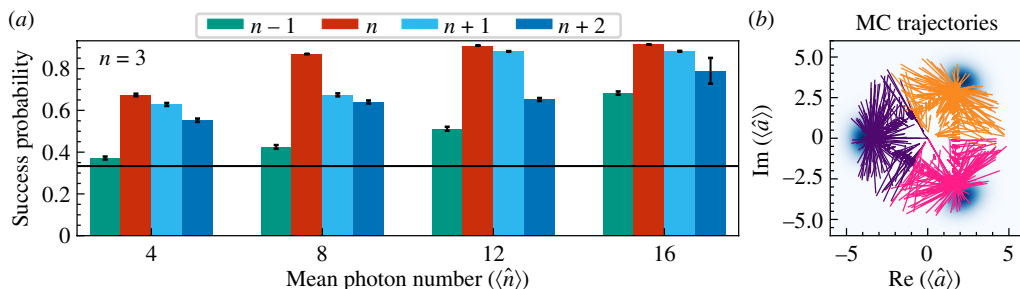


Figure 6. (a) Success probability for measuring the correct lobe starting from an initial squeezed-coherent state with random amplitude and squeezing parameter. The results are shown for different mean photon numbers of the lobes and dissipation powers (m) with fixed $n = 3$. Each bar is obtained from an average of over 500 Monte Carlo trajectories with different initial states. We include a horizontal black line that represents the success probability you would obtain by random guessing the lobe, that is, $1/n$. An example of such trajectories can be seen in (b) for the particular case (3, 4) with $\langle \hat{n} \rangle = 8$. The colours indicate the most similar lobe at $t = 0$.

towards the closest lobe (representing one of the stored memories) and remain there for a long time. Consequently, we can extract information about the corresponding lobe by measuring the state within this regime.

As an example, in figure 5, we show the time evolution of an initial squeezed-coherent state with a larger amplitude than the lobes. In the panels figure 5a–e, we see the Wigner distribution of such a state at specific times, and in figure 5f, the evolution of the imaginary part of the annihilation operator \hat{a} (left axis) characterizing approximately the amplitude of the state and the Mandel's Q parameter (right axis, see equation (5.1)) characterizing the squeezing.

We can see that the state undergoes three different dynamical regimes. First, an initial decay that kills all Liouvillian modes outside the metastable manifold (see figure 5a,b). The amplitude of the state decays to the amplitude of the lobes, and the Mandel parameter goes from super-Poissonian to sub-Poissonian. The dynamics then freeze, and the state remains for a long time in one of the metastable phases (see figure 5c,d). Finally, the metastable modes decay, and the steady state corresponding to figure 4a is reached in figure 5e.

We assess the QAM efficiency by numerically computing the probability that the system is found in the target lobe during the metastable phase. We initialize the system at a random squeezed-coherent state which, by definition, is most similar to one of the n lobes that constitute our system. Hence, the task succeeds if during the metastable phase, the state converges to the a prior correct lobe. The results of the success probability for the particular case $n = 3$ can be seen in figure 6 where we compare different levels of squeezing in the memories (different m) and increasing mean photon number of the lobes (larger separation).

We appreciate that the largest success probability is achieved in the case $n = m$, i.e. the memories are coherent states. Nevertheless, a high success probability can be achieved by a resonator with $m = n + 1$, which stores the memories in amplitude-squeezed states. This behaviour, however, is not general as for $n = 2$, a higher success probability is achieved with squeezed states instead of coherent states [68]. When storing more patterns ($n > 2$), one must take into account that the overlap between lobes decreases, so a larger mean photon number is needed to correctly discriminate the patterns. Still, as we can see in figure 6b, for a sufficiently large mean photon number, the phase space is divided into three distinct regions containing all the initial conditions that converge to the lobe inside it.

The possibility to experimentally realize resonators with high nonlinearities represents an important breakthrough to implement these tasks in actual devices in the near future [166,167]. We believe these types of resonators offer a high versatility to be used for numerous kinds of tasks such as QAM [68,146], autonomous quantum error correction [63,66] or quantum annealing [76,77].

6. Conclusions

Quantum optical networks, which are emerging in various contexts (from integrated photonics to the quantum internet), have the potential to enhance capabilities in communication, computation and ML. In the latter, they can exploit the advantages of both classical and quantum optics, namely energy efficiency, high speed, noise immunity, as well as access to a large Hilbert space (with the potential for an exponential increase in expressivity) and to quantum inputs and tasks. In particular, quantum photonics offers several advantages, including enhanced computational power through quantum computing, secure communication via quantum cryptography and highly sensitive detection capabilities for various applications in imaging and sensing.

These neuro-inspired computational methods hold great promise for both feed-forward circuits and recurrent neural network designs. Here, we have focused on two approaches, QRC and associative memories, highlighting the transformative impact of quantum optics in this field and shedding light on the role of the quantum property of squeezing to achieve improved performance.

In the case of QRC, we have illustrated how squeezing increases the range of applicability in realistic (noisy) scenarios. In fact, multimode squeezing enhances the memory available to the system and, as a result, improves performance in several benchmark temporal tasks. As for QAM, the introduction of squeezing extends the range of potential solutions for stored patterns to include genuine quantum objects that could not be stored efficiently in classical devices. Moving from a single oscillator to an array will enable storing and retrieving more quantum features, including entangled memories.

These results highlight the potential of using quantum optical techniques to make a paradigm shift in computational methods [146,168], paving the way for future innovations in a wide range of fields. By integrating concepts such as squeezing into the design of neural networks, we can achieve significant improvements in efficiency and capability, offering new solutions to complex problems.

Data accessibility. This article has no additional data.

Declaration of AI use. We have not used AI-assisted technologies in creating this article.

Authors' contributions. A.L.M.: investigation, methodology, software, writing—original draft, writing—review and editing; J.G.-B.: investigation, methodology, software, writing—original draft, writing—review and editing; G.L.G.: project administration, supervision, writing—original draft, writing—review and editing; M.C.S.: project administration, supervision, writing—original draft, writing—review and editing; R.Z.: investigation, project administration, supervision, writing—original draft, writing—review and editing.

All authors gave final approval for publication and agreed to be held accountable for the work performed therein.

Conflict of interest declaration. We declare we have no competing interests.

Funding. We acknowledge the Spanish State Research Agency, through the Maria de Maeztu project CEX2021-001164-M funded by the MCIN/AEI/10.13039/501100011033, through the COQUSY project PID2022-140506NB-C21 and -C22 funded by MCIN/AEI/10.13039/501100011033 and through the INFOLANET project PID2022-139409NB-I00 funded by MCIN/AEI/10.13039/501100011033; MINECO through the QUANTUM SPAIN project and EU through the RTRP - NextGenerationEU within the framework of the Digital Spain 2025 Agenda. G.L.G. is funded by the Spanish Ministerio de Educacion y Formacion Profesional/Ministerio de Universidades and co-funded by the University of the Balearic Islands through the Beatriz Galindo program (BG20/00085). A.L.M. is funded by the University of the Balearic Islands through the project BGRH-UIB-2021. J.G.B. is funded by the Conselleria d'Educació, Universitat i Recerca of the Government of the Balearic Islands with grant code FPI/036/2020.

Acknowledgements. This work is dedicated to Rodney Loudon, in memory of his enduring contributions to the field of quantum optics and of his kindness and elegance in research.

1. Loudon R. 1973 The Quantum Theory of Light. Oxford science publications. In *The quantum theory of light*, 3rd Edition. OUP Oxford.
2. O'Brien JL, Furusawa A, Vučković J. 2009 Photonic quantum technologies. *Nat. Photonics* **3**, 687–695. (doi:10.1038/nphoton.2009.229)
3. Benyoucef M (ed). 2023 *Photonic quantum technologies*. Weinheim, Germany: John Wiley & Sons, Ltd.
4. Pelucchi E *et al.* 2021 The potential and global outlook of integrated photonics for quantum technologies. *Nat. Rev. Phys.* **4**, 194–208. (doi:10.1038/s42254-021-00398-z)
5. Shadbolt P, Mathews JCF, Laing A, O'Brien JL. 2014 Testing foundations of quantum mechanics with photons. *Nat. Phys.* **10**, 278–286. (doi:10.1038/nphys2931)
6. Loudon R, Knight PL. 1987 Squeezed Light. *J. Mod. Opt.* **34**, 709–759. (doi:10.1080/09500348714550721)
7. Slusher RE, Hollberg LW, Yurke B, Mertz JC, Valley JF. 1985 Observation of squeezed states generated by four-wave mixing in an optical cavity. *Phys. Rev. Lett.* **55**, 2409–2412. (doi:10.1103/PhysRevLett.55.2409)
8. Giovannetti V, Lloyd S, Maccone L. 2004 Quantum-Enhanced Measurements: Beating the Standard Quantum Limit. *Science* **306**, 1330–1336. (doi:10.1126/science.1104149)
9. Ganapathy D *et al.* 2023 Broadband Quantum Enhancement of the LIGO Detectors with Frequency-Dependent Squeezing. *Phys. Rev. X* **13**, 041021. (doi:10.1103/physrevx.13.041021)
10. Aspect A, Dalibard J, Roger G. 1982 Experimental Test of Bell's Inequalities Using Time-Varying Analyzers. *Phys. Rev. Lett.* **49**, 1804–1807. (doi:10.1103/physrevlett.49.1804)
11. Fabre C, Treps N. 2020 Modes and states in quantum optics. *Rev. Mod. Phys.* **92**, 035005. (doi:10.1103/revmodphys.92.035005)
12. Argyris A *et al.* 2005 Chaos-based communications at high bit rates using commercial fibre-optic links. *Nature* **438**, 343–346. (doi:10.1038/nature04275)
13. Nokkala J, Piilo J, Bianconi G. 2024 Complex quantum networks: a topical review. *J. Phys.* **57**, 233001. (doi:10.1088/1751-8121/ad41a6)
14. Kolobov MI. 2007 *Quantum imaging*. New York: Springer.
15. Diddams SA, Vahala K, Udem T. 2020 Optical frequency combs: Coherently uniting the electromagnetic spectrum. *Science* **369**, y3676. (doi:10.1126/science.aay3676)
16. Roslund J, de Araújo RM, Jiang S, Fabre C, Treps N. 2014 Wavelength-multiplexed quantum networks with ultrafast frequency combs. *Nat. Photonics* **8**, 109–112. (doi:10.1038/nphoton.2013.340)
17. Reimer C *et al.* 2016 Generation of multiphoton entangled quantum states by means of integrated frequency combs. *Science* **351**, 1176–1180. (doi:10.1126/science.aad8532)
18. Cai Y, Roslund J, Ferrini G, Arzani F, Xu X, Fabre C, Treps N. 2017 Multimode entanglement in reconfigurable graph states using optical frequency combs. *Nat. Commun.* **8**, 15645. (doi:10.1038/ncomms15645)
19. Brod DJ, Galvão EF, Crespi A, Osellame R, Spagnolo N, Sciarrino F. 2019 Photonic implementation of boson sampling: a review. *Adv. Photon.* **1**, 034001.
20. Wang J, Sciarrino F, Laing A, Thompson MG. 2020 Integrated photonic quantum technologies. *Nat. Photonics* **14**, 273–284. (doi:10.1038/s41566-019-0532-1)
21. Eisert J, Hangleiter D, Walk N, Roth I, Markham D, Parekh R, Chabaud U, Kashefi E. 2020 Quantum certification and benchmarking. *Nat. Rev. Phys.* **2**, 382–390. (doi:10.1038/s42254-020-0186-4)
22. Aolita L, Gogolin C, Kliesch M, Eisert J. 2015 Reliable quantum certification of photonic state preparations. *Nat. Commun.* **6**, 8498. (doi:10.1038/ncomms9498)
23. Wang NN, Pozas-Kerstjens A, Zhang C, Liu BH, Huang YF, Li CF, Guo GC, Gisin N, Tavakoli A. 2023 Certification of non-classicality in all links of a photonic star network without assuming quantum mechanics. *Nat. Commun.* **14**, 2153. (doi:10.1038/s41467-023-37842-w)
24. Šupić I, Bowles J, Renou MO, Acín A, Hoban MJ. 2023 Quantum networks self-test all entangled states. *Nat. Phys.* **19**, 670–675. (doi:10.1038/s41567-023-01945-4)

25. Manzano G, Galve F, Giorgi GL, Hernández-García E, Zambrini R. 2013 Synchronization, quantum correlations and entanglement in oscillator networks. *Sci. Rep.* **3**, 1439. (doi:10.1038/srep01439)
26. Zambrini R, Hoyuelos M, Gatti A, Colet P, Lugiato L, San Miguel M. 2000 Quantum fluctuations in a continuous vectorial Kerr *medium* model. *Phys. Rev.* **62**, 063801. (doi:10.1103/physreva.62.063801)
27. Giorgi GL, Galve F, Manzano G, Colet P, Zambrini R. 2012 Quantum correlations and mutual synchronization. *Phys. Rev.* **85**, 052101. (doi:10.1103/physreva.85.052101)
28. Cabot A, Galve F, Eguíluz VM, Klemm K, Maniscalco S, Zambrini R. 2018 Unveiling noiseless clusters in complex quantum networks. *Npj Quantum Inf.* **4**. (doi:10.1038/s41534-018-0108-9)
29. Cabot A, Giorgi GL, Zambrini R. 2021 Metastable quantum entrainment. *New J. Phys.* **23**, 103017. (doi:10.1088/1367-2630/ac29fe)
30. Else DV, Bauer B, Nayak C. 2016 Floquet Time Crystals. *Phys. Rev. Lett.* **117**, 090402. (doi:10.1103/PhysRevLett.117.090402)
31. Iemini F, Russomanno A, Keeling J, Schirò M, Dalmonte M, Fazio R. 2018 Boundary Time Crystals. *Phys. Rev. Lett.* **121**, 035301. (doi:10.1103/PhysRevLett.121.035301)
32. Cabot A, Giorgi GL, Zambrini R. 2024 Nonequilibrium transition between a continuous and a discrete time-crystal. *PRX Quantum* **5**, 030325. (doi:10.1103/PRXQuantum.5.030325)
33. Vasile R, Galve F, Zambrini R. 2014 Spectral origin of non-Markovian open-system dynamics: A finite harmonic model without approximations. *Phys. Rev.* **89**, 022109. (doi:10.1103/physreva.89.022109)
34. Nokkala J, Arzani F, Galve F, Zambrini R, Maniscalco S, Piilo J, Treps N, Parigi V. 2018 Reconfigurable optical implementation of quantum complex networks. *New J. Phys.* **20**, 053024. (doi:10.1088/1367-2630/aabc77)
35. Renault P, Nokkala J, Roeland G, Joly NY, Zambrini R, Maniscalco S, Piilo J, Treps N, Parigi V. 2023 Experimental Optical Simulator of Reconfigurable and Complex Quantum Environment. *PRX Quantum* **4**, 040310. (doi:10.1103/prxquantum.4.040310)
36. Wehner S, Elkouss D, Hanson R. 2018 Quantum internet: A vision for the road ahead. *Science* **362**, eaam9288. (doi:10.1126/science.aam9288)
37. Kimble HJ. 2008 The quantum internet. *Nature* **453**, 1023–1030. (doi:10.1038/nature07127)
38. Shor PW, Preskill J. 2000 Simple proof of security of the BB84 quantum key distribution protocol. *Phys. Rev. Lett.* **85**, 441–444. (doi:10.1103/PhysRevLett.85.441)
39. Zhang Z, Zhuang Q. 2021 Distributed quantum sensing. *Quantum Sci. Technol.* **6**, 043001. (doi:10.1088/2058-9565/abd4c3)
40. Cirac JJ, Ekert AK, Huelga SF, Macchiavello C. 1999 Distributed quantum computation over noisy channels. *Phys. Rev.* **59**, 4249–4254. (doi:10.1103/physreva.59.4249)
41. Wootters WK, Zurek WH. 1982 A single quantum cannot be cloned. *Nature* **299**, 802–803. (doi:10.1038/299802a0)
42. Azuma K, Tamaki K, Lo HK. 2015 All-photonic quantum repeaters. *Nat. Commun.* **6**, 6787. (doi:10.1038/ncomms7787)
43. Weedbrook C, Pirandola S, García-Patrón R, Cerf NJ, Ralph TC, Shapiro JH, Lloyd S. 2012 Gaussian quantum information. *Rev. Mod. Phys.* **84**, 621–669. (doi:10.1103/RevModPhys.84.621)
44. Laudenbach F, Pacher C, Fung CF, Poppe A, Peev M, Schrenk B, Hentschel M, Walther P, Hübel H. 2018 Continuous - Variable Quantum Key Distribution with Gaussian Modulation—The Theory of Practical Implementations. *Adv. Quantum Technol.* **1**, 00011. (doi:10.1002/qute.201800011)
45. Cerf NJ, Lévy M, Assche GV. 2001 Quantum distribution of Gaussian keys using squeezed states. *Phys. Rev.* **63**, 052311. (doi:10.1103/physreva.63.052311)
46. Gottesman D, Preskill J. 2003 Secure Quantum Key Distribution using Squeezed States. In *Quantum information with continuous variables*, pp. 317–356. Springer Netherlands. (doi:10.1007/978-94-015-1258-9_22)
47. Pirandola S, García-Patrón R, Braunstein SL, Lloyd S. 2009 Direct and Reverse Secret-Key Capacities of a Quantum Channel. *Phys. Rev. Lett.* **102**, 050503. (doi:10.1103/PhysRevLett.102.050503)
48. Deutsch DE. 1989 Quantum computational networks. *Proc. R. Soc. Lond. A* **425**, 73–90.

49. Buluta I, Nori F. 2009 Quantum simulators. *Science* **326**, 108–111. (doi:10.1126/science.1177838)
50. Kendon VM, Nemoto K, Munro WJ. 2010 Quantum analogue computing. *Philos. Trans. R. Soc. A* **368**, 3609–3620. (doi:10.1098/rsta.2010.0017)
51. Walmsley I. 2023 Light in quantum computing and simulation: perspective. *Opt. Quantum* **1**, 35. (doi:10.1364/opticaq.507527)
52. Aspuru-Guzik A, Walther P. 2012 Photonic quantum simulators. *Nat. Phys.* **8**, 285–291. (doi:10.1038/nphys2253)
53. O’Brien JL. 2007 Optical quantum computing. *Science* **318**, 1567–1570. (doi:10.1126/science.1142892)
54. Gu M, Weedbrook C, Menicucci NC, Ralph TC, van Loock P. 2009 Quantum computing with continuous-variable clusters. *Phys. Rev.* **79**, 062318. (doi:10.1103/physreva.79.062318)
55. Yoshikawa J, Yokoyama S, Kaji T, Sornphiphatphong C, Shiozawa Y, Makino K, Furusawa A. 2016 Invited Article: Generation of one-million-mode continuous-variable cluster state by unlimited time-domain multiplexing. *APL Photonics* **1**, 4962732. (doi:10.1063/1.4962732)
56. Chen M, Menicucci NC, Pfister O. 2014 Experimental Realization of Multipartite Entanglement of 60 Modes of a Quantum Optical Frequency Comb. *Phys. Rev. Lett.* **112**, 120505. (doi:10.1103/PhysRevLett.112.120505)
57. Asavanant W *et al.* 2019 Generation of time-domain-multiplexed two-dimensional cluster state. *Science* **366**, 373–376. (doi:10.1126/science.aay2645)
58. Larsen MV, Guo X, Breum CR, Neergaard-Nielsen JS, Andersen UL. 2021 Deterministic multi-mode gates on a scalable photonic quantum computing platform. *Nat. Phys.* **17**, 1018–1023. (doi:10.1038/s41567-021-01296-y)
59. Asavanant W *et al.* 2021 Time-Domain-Multiplexed Measurement-Based Quantum Operations with 25-MHz Clock Frequency. *Phys. Rev. Appl.* **16**, 034005. (doi:10.1103/physrevapplied.16.034005)
60. Kozłowski W, Wehner S. 2019 Towards Large-Scale Quantum Networks. In *Proceedings of the sixth annual ACM international conference on nanoscale computing and communication*, pp. 1–7. New York, NY, USA. (doi:10.1145/3345312.3345497). <https://dl.acm.org/doi/proceedings/10.1145/3345312>.
61. Takeda S, Mizuta T, Fuwa M, van Loock P, Furusawa A. 2013 Deterministic quantum teleportation of photonic quantum bits by a hybrid technique. *Nature* **500**, 315–318. (doi:10.1038/nature12366)
62. Fowler AG, Mariantoni M, Martinis JM, Cleland AN. 2012 Surface codes: Towards practical large-scale quantum computation. *Phys. Rev.* **86**, 032324. (doi:10.1103/physreva.86.032324)
63. Cai W, Ma Y, Wang W, Zou CL, Sun L. 2021 Bosonic quantum error correction codes in superconducting quantum circuits. *Fundam. Res.* **1**, 50–67. (doi:10.1016/j.fmre.2020.12.006)
64. Campagne-Ibarcq P *et al.* 2020 Quantum error correction of a qubit encoded in grid states of an oscillator. *Nature* **584**, 368–372. (doi:10.1038/s41586-020-2603-3)
65. Hu L *et al.* 2019 Quantum error correction and universal gate set operation on a binomial bosonic logical qubit. *Nat. Phys.* **15**, 503–508. (doi:10.1038/s41567-018-0414-3)
66. Mirrahimi M, Leghtas Z, Albert VV, Touzard S, Schoelkopf RJ, Jiang L, Devoret MH. 2014 Dynamically protected cat-qubits: a new paradigm for universal quantum computation. *New J. Phys.* **16**, 045014. (doi:10.1088/1367-2630/16/4/045014)
67. Lescanne R, Villiers M, Peronnin T, Sarlette A, Delbecq M, Huard B, Kontos T, Mirrahimi M, Leghtas Z. 2020 Exponential suppression of bit-flips in a qubit encoded in an oscillator. *Nat. Phys.* **16**, 509–513. (doi:10.1038/s41567-020-0824-x)
68. Labay-Mora A, Zambrini R, Giorgi GL. 2024 Quantum memories for squeezed and coherent superpositions in a driven-dissipative nonlinear oscillator. *Phys. Rev.* **109**, 032407. (doi:10.1103/physreva.109.032407)
69. Aaronson S, Arkhipov A. 2013 The Computational Complexity of Linear Optics. *Theory Comput.* **9**, 143–252. (doi:10.4086/toc.2013.v009a004)
70. Hamilton CS, Kruse R, Sansoni L, Barkhofen S, Silberhorn C, Jex I. 2017 Gaussian Boson Sampling. *Phys. Rev. Lett.* **119**, 170501. (doi:10.1103/PhysRevLett.119.170501)

71. Wang H *et al.* 2019 Boson Sampling with 20 Input Photons and a 60-Mode Interferometer in a 10^{14} Dimensional Hilbert Space. *Phys. Rev. Lett.* **123**, 250503. (doi:10.1103/PhysRevLett.123.250503)
72. Zhong HS *et al.* 2020 Quantum computational advantage using photons. *Science* **370**, 1460–1463. (doi:10.1126/science.abe8770)
73. Madsen LS *et al.* 2022 Quantum computational advantage with a programmable photonic processor. *Nature* **606**, 75–81. (doi:10.1038/s41586-022-04725-x)
74. McMahon PL *et al.* 2016 A fully programmable 100-spin coherent Ising machine with all-to-all connections. *Science* **354**, 614–617. (doi:10.1126/science.aah5178)
75. Honjo T *et al.* 2021 100,000-spin coherent Ising machine. *Sci. Adv.* **7**, eabh0952. (doi:10.1126/sciadv.abh0952)
76. Puri S, Andersen CK, Grimsmo AL, Blais A. 2017 Quantum annealing with all-to-all connected nonlinear oscillators. *Nat. Commun.* **8**, 15785. (doi:10.1038/ncomms15785)
77. Nigg SE, Lörch N, Tiwari RP. 2017 Robust quantum optimizer with full connectivity. *Sci. Adv.* **3**, e1602273. (doi:10.1126/sciadv.1602273)
78. Peruzzo A, McClean J, Shadbolt P, Yung MH, Zhou XQ, Love PJ, Aspuru-Guzik A, O'Brien JL. 2014 A variational eigenvalue solver on a photonic quantum processor. *Nat. Commun.* **5**, 4213. (doi:10.1038/ncomms5213)
79. Genty G, Salmela L, Dudley JM, Brunner D, Kokhanovskiy A, Kobtsev S, Turitsyn SK. 2021 Machine learning and applications in ultrafast photonics. *Nat. Photonics* **15**, 91–101. (doi:10.1038/s41566-020-00716-4)
80. Wiecha PR, Arbouet A, Girard C, Muskens OL. 2021 Deep learning in nano-photonics: inverse design and beyond. *Photon. Res.* **9**, B182. (doi:10.1364/PRJ.415960)
81. Fu X, Kutz JN. 2013 High-energy mode-locked fiber lasers using multiple transmission filters and a genetic algorithm. *Opt. Express* **21**, 6526–6537. (doi:10.1364/OE.21.006526)
82. Ma W, Liu Z, Kudyshev ZA, Boltasseva A, Cai W, Liu Y. 2021 Deep learning for the design of photonic structures. *Nat. Photonics* **15**, 77–90. (doi:10.1038/s41566-020-0685-y)
83. Krenn M, Malik M, Fickler R, Lapkiewicz R, Zeilinger A. 2016 Automated Search for new Quantum Experiments. *Phys. Rev. Lett.* **116**, 090405. (doi:10.1103/PhysRevLett.116.090405)
84. Krenn M, Hochrainer A, Lahiri M, Zeilinger A. 2017 Entanglement by Path Identity. *Phys. Rev. Lett.* **118**, 080401. (doi:10.1103/PhysRevLett.118.080401)
85. Cervera-Lierta A, Krenn M, Aspuru-Guzik A. 2022 Design of quantum optical experiments with logic artificial intelligence. *Quantum* **6**, 836. (doi:10.22331/q-2022-10-13-836)
86. Krenn M, Kottmann JS, Tischler N, Aspuru-Guzik A. 2021 Conceptual Understanding through Efficient Automated Design of Quantum Optical Experiments. *Phys. Rev. X* **11**, 031044. (doi:10.1103/physrevx.11.031044)
87. Labay-Mora A, da Silva FF, Wehner S. 2024 Reducing hardware requirements for entanglement distribution via joint hardware-protocol optimization. *Quantum Sci. Technol.* **9**, 045001. (doi:10.1088/2058-9565/ad57e9)
88. Avis G, Ferreira da Silva F, Coopmans T, Dahlberg A, Jirovská H, Maier D, Rabbie J, Torres-Knoop A, Wehner S. 2023 Requirements for a processing-node quantum repeater on a real-world fiber grid. *Npj Quantum Inf.* **9**, 100. (doi:10.1038/s41534-023-00765-x)
89. Mafu M. 2024 Advances in artificial intelligence and machine learning for quantum communication applications. *IET Quantum Commun.* **5**, 202–231. (doi:10.1049/qt2.12094)
90. Torlai G, Mazzola G, Carrasquilla J, Troyer M, Melko R, Carleo G. 2018 Neural-network quantum state tomography. *Nat. Phys.* **14**, 447–450. (doi:10.1038/s41567-018-0048-5)
91. Koutný D, Ginés L, Moczała-Dusanowska M, Höfling S, Schneider C, Predojević A, Ježek M. 2023 Deep learning of quantum entanglement from incomplete measurements. *Sci. Adv.* **9**, eadd7131. (doi:10.1126/sciadv.add7131)
92. Goy A, Arthur K, Li S, Barbastathis G. 2018 Low Photon Count Phase Retrieval Using Deep Learning. *Phys. Rev. Lett.* **121**, 243902. (doi:10.1103/PhysRevLett.121.243902)
93. McMahon PL. 2023 The physics of optical computing. *Nat. Rev. Phys.* **5**, 717–734. (doi:10.1038/s42254-023-00645-5)
94. Won R. 2023 The power of light-driven computing. *Nat. Photonics* **17**, 934–936. (doi:10.1038/s41566-023-01323-9)
95. Shen Y *et al.* 2017 Deep learning with coherent nanophotonic circuits. *Nat. Photonics* **11**, 441–446. (doi:10.1038/nphoton.2017.93)

96. Lin X, Rivenson Y, Yardimci NT, Veli M, Luo Y, Jarrahi M, Ozcan A. 2018 All-optical machine learning using diffractive deep neural networks. *Science* **361**, 1004–1008. (doi:10.1126/science.aat8084)
97. Sui X, Wu Q, Liu J, Chen Q, Gu G. 2020 A Review of Optical Neural Networks. *IEEE Access* **8**, 70773–70783. (doi:10.1109/access.2020.2987333)
98. Wetzstein G, Ozcan A, Gigan S, Fan S, Englund D, Soljačić M, Denz C, Miller DAB, Psaltis D. 2020 Inference in artificial intelligence with deep optics and photonics. *Nature* **588**, 39–47. (doi:10.1038/s41586-020-2973-6)
99. Shastri BJ, Tait AN, Ferreira de Lima T, Pernice WHP, Bhaskaran H, Wright CD, Prucnal PR. 2021 Photonics for artificial intelligence and neuromorphic computing. *Nat. Photonics* **15**, 102–114. (doi:10.1038/s41566-020-00754-y)
100. Harris NC *et al.* 2018 Linear programmable nanophotonic processors. *Optica* **5**, 1623. (doi:10.1364/optica.5.001623)
101. Matuszewski M, Prystupniuk A, Opala A. 2024 Role of all-optical neural networks. *Phys. Rev. Appl.* **21**, 014028. (doi:10.1103/PhysRevApplied.21.014028)
102. Hamerly R, Bernstein L, Sludds A, Soljačić M, Englund D. 2019 Large-Scale Optical Neural Networks Based on Photoelectric Multiplication. *Phys. Rev. X* **9**, 021032. (doi:10.1103/physrevx.9.021032)
103. Basani JR, Heuck M, Englund DR, Krastanov S. 2024 All-photonic artificial-neural-network processor via nonlinear optics. *Phys. Rev. Appl.* **22**. (doi:10.1103/PhysRevApplied.22.014009)
104. Ashtiani F, Geers AJ, Aflatouni F. 2022 An on-chip photonic deep neural network for image classification. *Nature* **606**, 501–506. (doi:10.1038/s41586-022-04714-0)
105. Wan KH, Dahlsten O, Kristjánsson H, Gardner R, Kim MS. 2017 Quantum generalisation of feedforward neural networks. *Npj Quantum Inf.* **3**. (doi:10.1038/s41534-017-0032-4)
106. Marković D, Grollier J. 2020 Quantum neuromorphic computing. *Appl. Phys. Lett.* **117**, 150501. (doi:10.1063/5.0020014)
107. Killoran N, Bromley TR, Arrazola JM, Schuld M, Quesada N, Lloyd S. 2019 Continuous-variable quantum neural networks. *Phys. Rev. Res.* **1**, 033063. (doi:10.1103/PhysRevResearch.1.033063)
108. Steinbrecher GR, Olson JP, Englund D, Carolan J. 2019 Quantum optical neural networks. *Npj. Quantum. Inf.* **5**, 60. (doi:10.1038/s41534-019-0174-7)
109. Cerezo M, Verdon G, Huang HY, Cincio L, Coles PJ. 2022 Challenges and opportunities in quantum machine learning. *Nat. Comput. Sci.* **2**, 567–576. (doi:10.1038/s43588-022-00311-3)
110. Jeswal SK, Chakraverty S. 2019 Recent Developments and Applications in Quantum Neural Network: A Review. *Arch. Comput. Methods Eng.* **26**, 793–807. (doi:10.1007/s11831-018-9269-0)
111. Parthasarathy R, Bhowmik RT. 2021 Quantum Optical Convolutional Neural Network: A Novel Image Recognition Framework for Quantum Computing. *IEEE Access* **9**, 103337–103346. (doi:10.1109/access.2021.3098775)
112. Ventura D. 2000 Quantum associative memory. *Inf. Sci.* **124**, 273–296. (doi:10.1016/s0020-0255(99)00101-2)
113. Quiroz G, Ice L, Delgado A, Humble TS. 2021 Particle track classification using quantum associative memory. *Nucl. Instruments Methods Phys. Res. Sect.* **1010**, 165557. (doi:10.1016/j.nima.2021.165557)
114. Shapoval I, Calafiura P. 2019 Quantum Associative Memory in Hep Track Pattern Recognition. *EPJ Web Conf.* (eds A Forti, L Betev, M Litmaath, O Smirnova, P Hristov), **214**, 01012. (doi:10.1051/epjconf/201921401012)
115. Nokkala J. 2023 Online quantum time series processing with random oscillator networks. *Sci. Rep.* **13**, 7694. (doi:10.1038/s41598-023-34811-7)
116. Prins RD, Sande GV, Bienstman P. 2023 *A quantum optical recurrent neural network for online processing of quantum times series.*
117. Mujal P, Martínez - Peña R, Nokkala J, García - Beni J, Giorgi GL, Soriano MC, Zambrini R. 2021 Opportunities in Quantum Reservoir Computing and Extreme Learning Machines. *Adv. Quantum Technol.* **4**, 00027. (doi:10.1002/qute.202100027)
118. Chen J, Nurdin HI, Yamamoto N. 2020 Temporal Information Processing on Noisy Quantum Computers. *Phys. Rev. Appl.* **14**, 024065. (doi:10.1103/PhysRevApplied.14.024065)

119. Fry D, Deshmukh A, Chen SYC, Rastunkov V, Markov V. 2023 Optimizing quantum noise-induced reservoir computing for nonlinear and chaotic time series prediction. *Sci. Rep.* **13**, 19326. (doi:10.1038/s41598-023-45015-4)
120. Domingo L, Carlo G, Borondo F. 2022 Optimal quantum reservoir computing for the noisy intermediate-scale quantum era. *Phys. Rev. E* **106**, L043301. (doi:10.1103/PhysRevE.106.L043301)
121. Fujii K, Nakajima K. 2017 Harnessing Disordered-Ensemble Quantum Dynamics for Machine Learning. *Phys. Rev. Appl.* **8**, 024030. (doi:10.1103/physrevapplied.8.024030)
122. Lukoševičius M, Jaeger H. 2009 Reservoir computing approaches to recurrent neural network training. *Comput. Sci. Rev.* **3**, 127–149. (doi:10.1016/j.cosrev.2009.03.005)
123. Nakajima K. 2020 Physical reservoir computing—an introductory perspective. *Jpn. J. Appl. Phys.* **59**, 060501. (doi:10.35848/1347-4065/ab8d4f)
124. Brunner D, Soriano MC, Van der Sande G. 2019 *Photonic reservoir computing: optical recurrent neural networks*. Berlin, Germany: Walter de Gruyter GmbH & Co KG.
125. Spagnolo M, Morris J, Piacentini S, Antesberger M, Massa F, Crespi A, Ceccarelli F, Osellame R, Walther P. 2022 Experimental photonic quantum memristor. *Nat. Photonics* **16**, 318–323. (doi:10.1038/s41566-022-00973-5)
126. Llodrà G, Charalambous C, Giorgi GL, Zambrini R. 2023 Benchmarking the Role of Particle Statistics in Quantum Reservoir Computing. *Adv. Quantum Technol.* **6**. (doi:10.1002/qute.202200100)
127. Dudas J, Carles B, Plouet E, Mizrahi FA, Grollier J, Marković D. 2023 Quantum reservoir computing implementation on coherently coupled quantum oscillators. *Npj Quantum Inf.* **9**. (doi:10.1038/s41534-023-00734-4)
128. Suprano A *et al.* 2024 Experimental Property Reconstruction in a Photonic Quantum Extreme Learning Machine. *Phys. Rev. Lett.* **132**, 160802. (doi:10.1103/PhysRevLett.132.160802)
129. Govia LCG, Ribeill GJ, Rowlands GE, Krovi HK, Ohki TA. 2021 Quantum reservoir computing with a single nonlinear oscillator. *Phys. Rev. Res.* **3**, 013077. (doi:10.1103/physrevresearch.3.013077)
130. Nokkala J, Martínez-Peña R, Giorgi GL, Parigi V, Soriano MC, Zambrini R. 2021 Gaussian states of continuous-variable quantum systems provide universal and versatile reservoir computing. *Commun. Phys.* **4**. (doi:10.1038/s42005-021-00556-w)
131. García-Beni J, Giorgi GL, Soriano MC, Zambrini R. 2023 Scalable Photonic Platform for Real-Time Quantum Reservoir Computing. *Phys. Rev. Appl.* **20**, 014051. (doi:10.1103/physrevapplied.20.014051)
132. García-Beni J, Luca Giorgi G, Soriano MC, Zambrini R. 2024 Squeezing as a resource for time series processing in quantum reservoir computing. *Opt. Express* **32**, 6733–6747. (doi:10.1364/OE.507684)
133. Angelatos G, Khan SA, Türeci HE. 2021 Reservoir Computing Approach to Quantum State Measurement. *Phys. Rev. X* **11**, 041062. (doi:10.1103/physrevx.11.041062)
134. Senanian A *et al.* 2024 Microwave signal processing using an analog quantum reservoir computer. *Nat. Commun.* **15**, 7490. (doi:10.1038/s41467-024-51161-8)
135. Hopfield JJ. 1982 Neural networks and physical systems with emergent collective computational abilities. *Proc. Natl Acad. Sci. USA* **79**, 2554–2558. (doi:10.1073/pnas.79.8.2554)
136. Amit DJ. 1989 *Modeling brain function: the world of attractor neural networks*. Cambridge University Press. (doi:10.1017/CBO9780511623257)
137. Inoue J ichi. 2011 Pattern-recalling processes in quantum Hopfield networks far from saturation. *J. Phys.* **297**, 012012. (doi:10.1088/1742-6596/297/1/012012)
138. Neigovzen R, Neves JL, Sollacher R, Glaser SJ. 2009 Quantum pattern recognition with liquid-state nuclear magnetic resonance. *Phys. Rev. A* **79**, 042321. (doi:10.1103/PhysRevA.79.042321)
139. Rotondo P, Marcuzzi M, Garrahan JP, Lesanovsky I, Müller M. 2018 Open quantum generalisation of Hopfield neural networks. *J. Phys.* **51**, 115301. (doi:10.1088/1751-8121/aaabcb)
140. Fiorelli E, Rotondo P, Marcuzzi M, Garrahan JP, Lesanovsky I. 2019 Quantum accelerated approach to the thermal state of classical all-to-all connected spin systems with applications

- to pattern retrieval in the Hopfield neural network. *Phys. Rev. A* **99**, 032126. (doi:10.1103/PhysRevA.99.032126)
141. Fiorelli E, Lesanovsky I, Müller M. 2022 Phase diagram of quantum generalized Potts-Hopfield neural networks. *New J. Phys.* **24**, 033012. (doi:10.1088/1367-2630/ac5490)
 142. Fiorelli E, Marcuzzi M, Rotondo P, Carollo F, Lesanovsky I. 2020 Signatures of Associative Memory Behavior in a Multimode Dicke Model. *Phys. Rev. Lett.* **125**, 070604. (doi:10.1103/physrevlett.125.070604)
 143. Marsh BP, Guo Y, Kroeze RM, Gopalakrishnan S, Ganguli S, Keeling J, Lev BL. 2021 Enhancing Associative Memory Recall and Storage Capacity Using Confocal Cavity QED. *Phys. Rev. X* **11**, 021048. (doi:10.1103/physrevx.11.021048)
 144. Bödeker L, Fiorelli E, Müller M. 2023 Optimal storage capacity of quantum Hopfield neural networks. *Phys. Rev. Res.* **5**, 023074. (doi:10.1103/PhysRevResearch.5.023074)
 145. Lewenstein M, Gratsea A, Riera-Campenay A, Aloy A, Kasper V, Sanpera A. 2021 Storage capacity and learning capability of quantum neural networks. *Quantum Sci. Technol.* **6**, 045002. (doi:10.1088/2058-9565/ac070f)
 146. Labay-Mora A, Zambrini R, Giorgi GL. 2023 Quantum Associative Memory with a Single Driven-Dissipative Nonlinear Oscillator. *Phys. Rev. Lett.* **130**, 190602. (doi:10.1103/PhysRevLett.130.190602)
 147. Giovannetti V, Lloyd S, Maccone L. 2001 Quantum-enhanced positioning and clock synchronization. *Nature* **412**, 417–419. (doi:10.1038/35086525)
 148. Madsen LS, Usenko VC, Lassen M, Filip R, Andersen UL. 2012 Continuous variable quantum key distribution with modulated entangled states. *Nat. Commun.* **3**, 1083. (doi:10.1038/ncomms2097)
 149. Mual P, Nokkala J, Martínez-Peña R, Giorgi GL, Soriano MC, Zambrini R. 2021 Analytical evidence of nonlinearity in qubits and continuous-variable quantum reservoir computing. *J. Phys.* **2**, 045008. (doi:10.1088/2632-072x/ac340e)
 150. Nokkala J, Martinez-Pena R, Zambrini R, Soriano MC. 2022 High-Performance Reservoir Computing With Fluctuations in Linear Networks. *IEEE Trans. Neural Networks Learn. Syst.* **33**, 2664–2675. (doi:10.1109/TNNLS.2021.3105695)
 151. Collett MJ, Loudon R, Gardiner CW. 1987 Quantum Theory of Optical Homodyne and Heterodyne Detection. *J. Mod. Opt.* **34**, 881–902. (doi:10.1080/09500348714550811)
 152. Serafini A. 2017 *Quantum continuous variables: a primer of theoretical methods*. Boca Raton, FL: CRC Press.
 153. Mual P, Martínez-Peña R, Giorgi GL, Soriano MC, Zambrini R. 2023 Time-series quantum reservoir computing with weak and projective measurements. *Npj Quantum Inf.* **9**. (doi:10.1038/s41534-023-00682-z)
 154. Braunstein SL. 2005 Squeezing as an irreducible resource. *Phys. Rev.* **71**, 055801. (doi:10.1103/physreva.71.055801)
 155. Cariolaro G, Pierobon G. 2016 Reexamination of Bloch-Messiah reduction. *Phys. Rev. A* **93**, 062115. (doi:10.1103/PhysRevA.93.062115)
 156. Hubner U, Abraham NB, Weiss CO. 1989 Dimensions and entropies of chaotic intensity pulsations in a single-mode far-infrared NH₃ laser. *Phys. Rev. A* **40**, 6354–6365. (doi:10.1103/PhysRevA.40.6354)
 157. Weigend A, Gershenfeld N. 1993 Results of the time series prediction competition at the Santa Fe Institute. In *IEEE International Conference on Neural Networks*, vol. 3, pp. 1786–1793. (doi:10.1109/ICNN.1993.298828)
 158. Tomoda H, Yoshida T, Kashiwazaki T, Umeki T, Enomoto Y, Takeda S. 2023 Programmable time-multiplexed squeezed light source. *Opt. Express* **31**, 2161. (doi:10.1364/oe.476025)
 159. Kouadou T, Sansavini F, Ansquer M, Henaff J, Treps N, Parigi V. 2023 Spectrally shaped and pulse-by-pulse multiplexed multimode squeezed states of light. *APL Photonics* **8**. (doi:10.1063/5.0156331)
 160. Cai Y, Roslund J, Thiel V, Fabre C, Treps N. 2021 Quantum enhanced measurement of an optical frequency comb. *Npj Quantum Inf.* **7**. (doi:10.1038/s41534-021-00419-w)
 161. Valdez MA, Jaschke D, Vargas DL, Carr LD. 2017 Quantifying Complexity in Quantum Phase Transitions via Mutual Information Complex Networks. *Phys. Rev. Lett.* **119**, 225301. (doi:10.1103/PhysRevLett.119.225301)

162. Sakurai A, Estarellas MP, Munro WJ, Nemoto K. 2022 Quantum Extreme Reservoir Computation Utilizing Scale-Free Networks. *Phys. Rev. Appl.* **17**, 064044. (doi:[10.1103/physrevapplied.17.064044](https://doi.org/10.1103/physrevapplied.17.064044))
163. Braunstein SL, McLachlan RI. 1987 Generalized squeezing. *Phys. Rev. A* **35**, 1659–1667. (doi:[10.1103/PhysRevA.35.1659](https://doi.org/10.1103/PhysRevA.35.1659))
164. Macieszczak K, Rose DC, Lesanovsky I, Garrahan JP. 2021 Theory of classical metastability in open quantum systems. *Phys. Rev. Res.* **3**, 033047. (doi:[10.1103/physrevresearch.3.033047](https://doi.org/10.1103/physrevresearch.3.033047))
165. Brinkman BAW, Yan H, Maffei A, Park IM, Fontanini A, Wang J, La Camera G. 2022 Metastable dynamics of neural circuits and networks. *Appl. Phys. Rev.* **9**, 011313. (doi:[10.1063/5.0062603](https://doi.org/10.1063/5.0062603))
166. Svensson IM, Bengtsson A, Bylander J, Shumeiko V, Delsing P. 2018 Period multiplication in a parametrically driven superconducting resonator. *Appl. Phys. Lett.* **113**, 022602. (doi:[10.1063/1.5026974](https://doi.org/10.1063/1.5026974))
167. Chang CWS, Sabín C, Forn-Díaz P, Quijandría F, Vadiraj AM, Nsanzineza I, Johansson G, Wilson CM. 2020 Observation of Three-Photon Spontaneous Parametric Down-Conversion in a Superconducting Parametric Cavity. *Phys. Rev. X* **10**, 011011. (doi:[10.1103/physrevx.10.011011](https://doi.org/10.1103/physrevx.10.011011))
168. García-Beni J, Paparelle I, Parigi V, Giorgi GL, Soriano MC, Zambrini R. 2024 Quantum machine learning via continuous-variable cluster states and teleportation. *arXiv*. (doi:[10.48550/arXiv.2411.06907](https://doi.org/10.48550/arXiv.2411.06907))